Comparing Physics-Informed Loss Functions for Porosity Prediction in Laser Metal Deposition

Presented by Erin McGowan
Mentor: Dr. Weihong (Grace) Guo

Laser Metal Deposition (LMD)

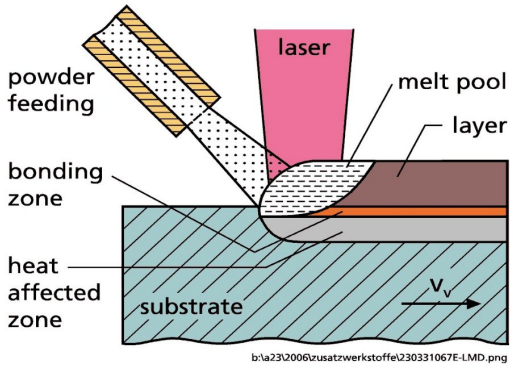

- Additive manufacturing (AM) technique in which a laser beam is used to fuse metal powder by melting it as it is deposited, layer by layer
- Used in automotive, aerospace, energy, petrochemicals, and medical industries
- Benefits:
  - High build-up rate and density
  - Very customizable
  - Reduces waste
  - Works for large components
  - Suitable for manufacturing and repair

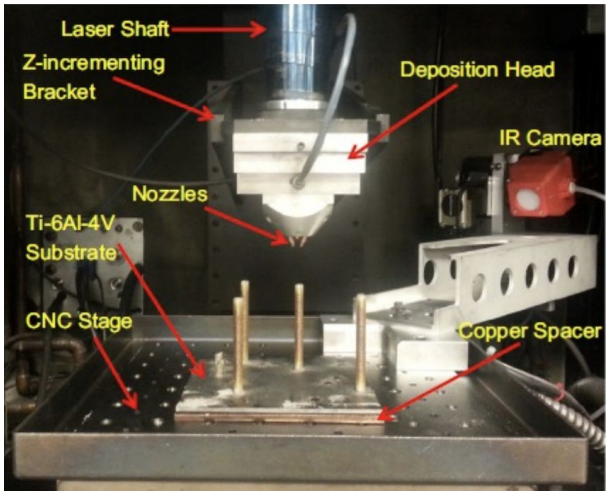

Porosity

- Occurs when tiny cavities form in the metal as it is printed
- Various causes (insufficient energy input, overheating, raw material defects)
- Can never be completely eliminated due to process instability
- Considered to be one of the most destructive defects in metal AM
    - Reduces static mechanical properties
    - Causes significant scatter of fatigue
- **Our goal:** predict whether parts printed via LMD will have a “good” (negligible) or “bad” (at least one pore ≥ 0.05mm diameter) level of porosity

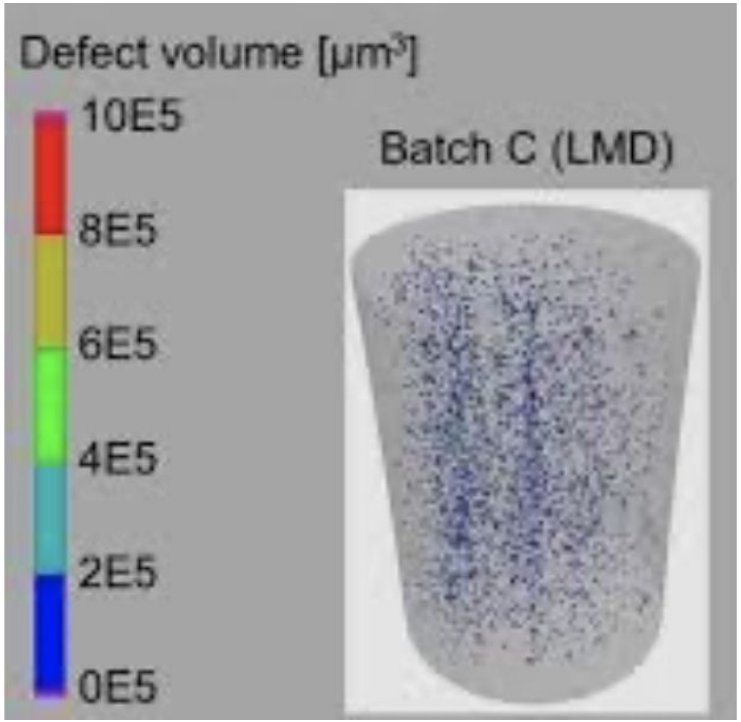

	Physics-Driven Approach Analytical and numerical models based on process mechanics	Data Science Approach Supervised learning methods that take in high-speed thermal images melt pools and put out a binary indicator of porosity
Advantages	• Useful for understanding the nature of pore formation and its characteristics	• Can predict porosity during LMD • Can handle complex data (high dimensionality, heterogeneity, large volume) • Efficient and accurate
Disadvantages	• Can have incomplete or missing physics • Requires calibration of model parameters • Computationally expensive • Lacks the ability of real-time prediction	• Black-box methods don't incorporate physics knowledge • Must be carefully trained with available experimental data • Difficult to interpret, apply, or generalize for a wider set of process conditions

Physics-Informed Deep Learning Model

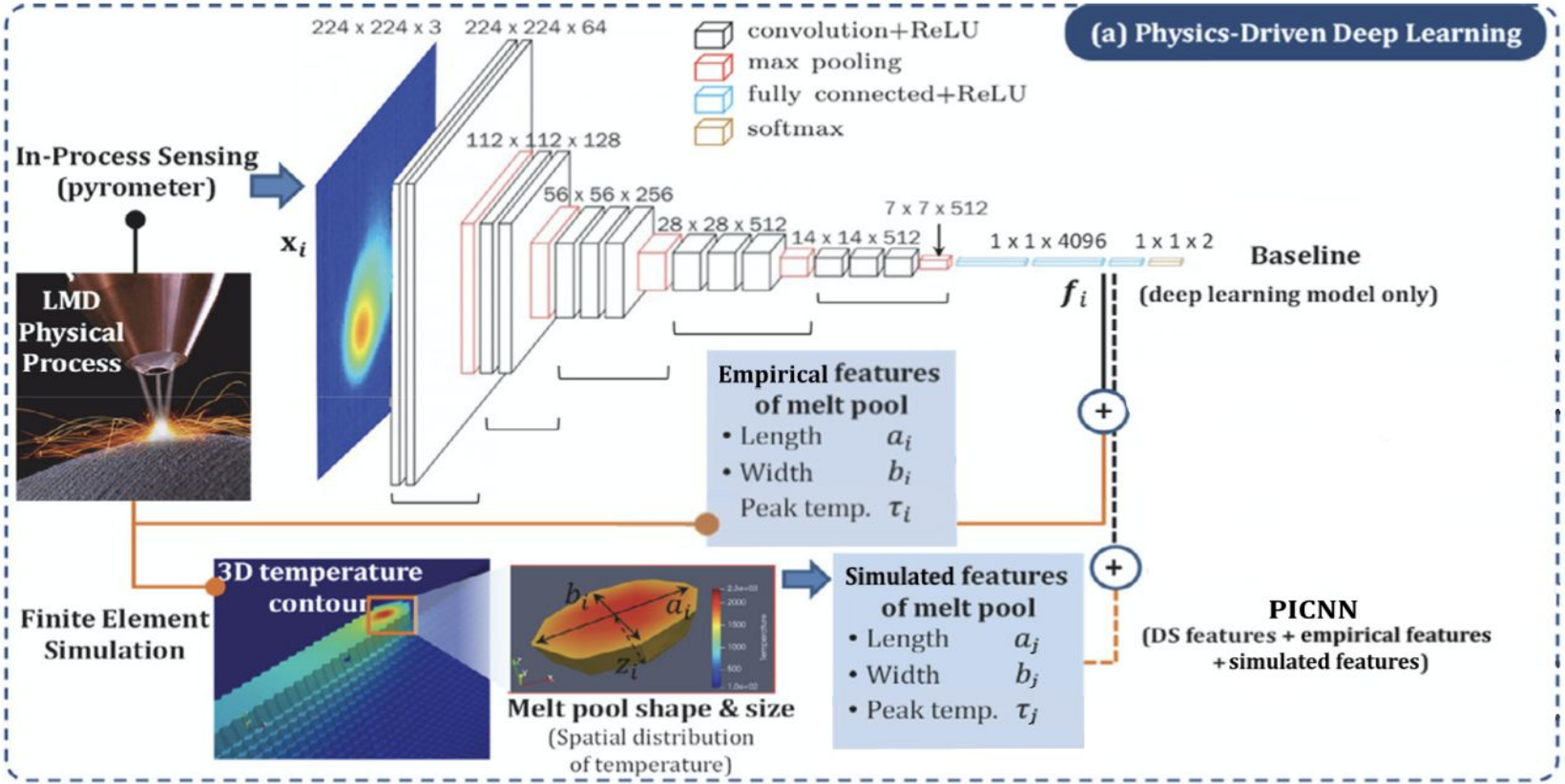

Fig. 4. Architecture of the proposed physics-driven deep learning model.

Adapted from W.''. Guo et al

Empirical LMD Data

- OPTOMEC LENSTM system with a 1Kw Nd: YAG laser was used to fabricate a thinwall structure from Ti-6Al-4V powders
- A dual-wavelength pyrometer and an infrared (IR) camera captured thermal data in real time
  - 1564 melt pool images across a total of 60 layers during a 457s LMD process
  - Each raw image was routed to a separate CSV file as a 752*480 matrix of temperatures (°C)
  - Images are temporally independent (pyrometer was vertically stationary relative to the melt pool)

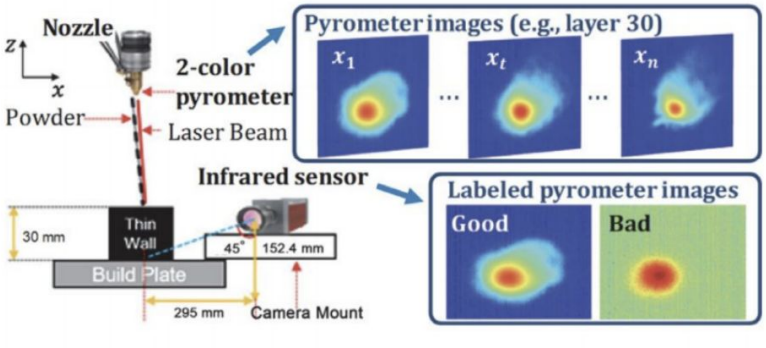

Figure 1: In-process sensing during LMD (left) and examples of pyrometer images (right) as seen in [2].

- True porosity measured by Micro-CT (3D imaging technique that uses x-rays to scan an object)
- Melt pool length and width were calculated by counting the number of pixels from the maximum temperature to the melting point in each direction

Simulated LMD Data

- A Finite Element Analysis (FEA) model was used to obtain simulated melt pool data [8]
  - maximum melt pool temperature
  - melt pool length
  - melt pool width
- Fig. 2 shows the model setup
- Each simulated melt pool was matched to an empirical melt pool based on similar time and part of print [8]

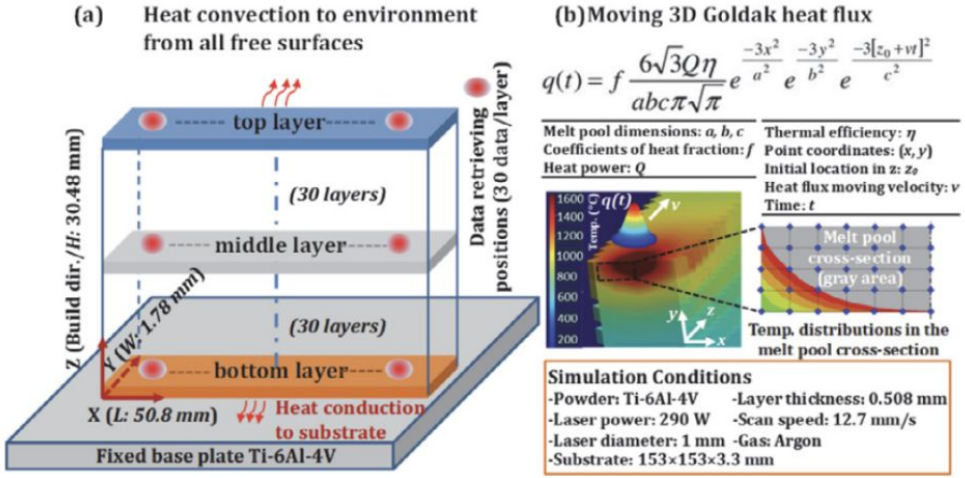

Figure 2: (a) FEA simulation structure (not to scale) and (b) Laser heat source model and thermal history of the melt pool as seen in [2].

Data Preprocessing

- Each empirical melt pool CSV file was converted into a 224x224 pixel RGB image centered around the maximum temperature location using Python, OpenCV, and PlantCV
- Images were labeled “bad” (at least one pore ≥ 0.05mm diameter) or “good” and split into training and test sets
    - 1486 “good” images, 71 “bad” images, 7 images that could not be clearly classified (latter removed for model training purposes)
- To account for class imbalance, “bad” training images were augmented (horizontal/vertical flips, brightness shifts) to create additional “bad” training data
    - Training set: 1237 “good” and 1237 “bad” images
    - Test set: 249 “good” and 12 “bad” images
- A validation set consisting of 15% of the training set (185 “good” and 185 “bad”) was then randomly portioned out

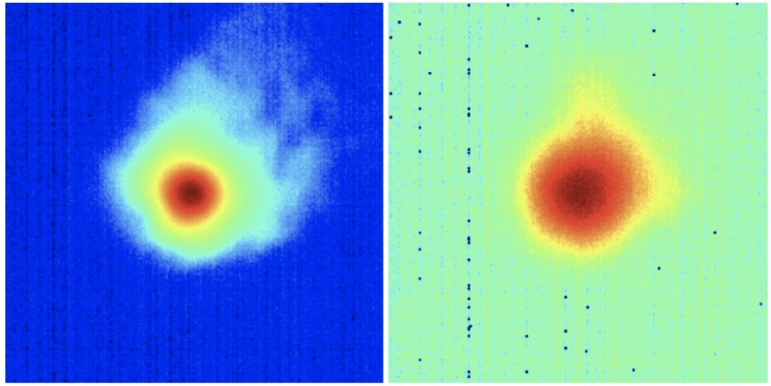

Figure 3: An example of a “good” pyrometer image (left) and a “bad” pyrometer image (right).

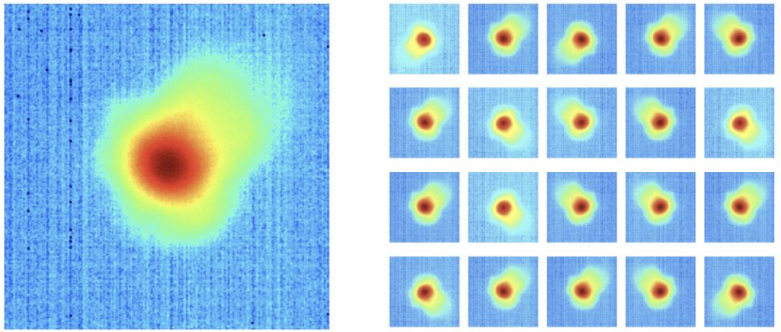

Figure 4: An example of a “bad” pyrometer image (left) and the 20 additional images created from it via bootstrapping methods (right).

Deep Learning Model Architecture (VGG16)

- VGG16 is a convolutional neural network (CNN), a type of neural network typically used to analyze images
- Proposed by K. Simonyan and A. Zisserman (University of Oxford) in 2014
- 92.7% accurate when completing a top-5 test in ImageNet, a dataset of over 14 million images that can be sorted into 1000 classes

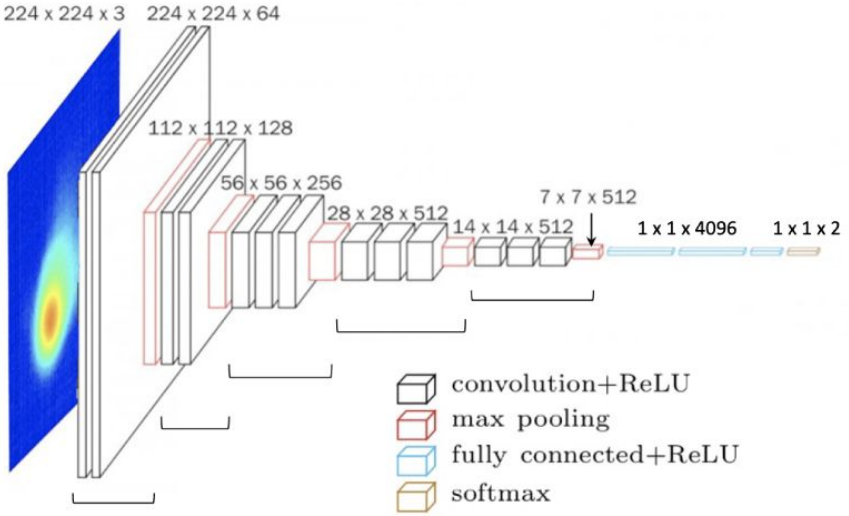

Fig. 5: The VGG16 Architecture

Physics-Informed Loss Functions

- Deep learning models seek to minimize loss and use loss functions to evaluate the discrepancy between the true (y_{true}) and predicted (y_{pred}) label for a given input
- Categorical cross entropy loss is a popular choice for classification models (including our baseline deep learning-only model)
  - Since we have two classes,

    CCELoss(ytrue, ypred) = $-t_1 \log(s_1) - (1 - t_1) * \log(1 - s_1)$,

    where t_1 and s_1 are the true label and predicted label for Class 1 and $(1 - t_1)$ and $(1 - s_1)$ are the true label and predicted label for Class 2
- Current research [4, 5] has shown that effective physics/deep learning hybrid models can be constructed by using physical data to influence or constrain the loss function

Physics-Informed Loss Functions (cont.)

Model	Loss Function
Deep Learning Only	$CCELoss(y_{true}, y_{pred})$
PICNN1	$CCELoss(y_{true}, y_{pred}) + \frac{1}{N}\sum_{i=1}^{N} ReLU(R)$
PICNN2	$CCELoss(y_{true}, y_{pred}) + \frac{1}{N}\sum_{i=1}^{N} ReLU(\frac{l}{w} - 1.1)$ $+\frac{1}{N}\sum_{i=1}^{N} ReLU((-1) * \frac{l}{w} - 0.9)$
PICNN3	$CCELoss(y_{true}, y_{pred})$ $+\lambda_t \times \frac{1}{N}\sum_{i=1}^{N} ReLU(\epsilon_t - 1.53658168)$
PICNN4	$CCELoss(y_{true}, y_{pred})$ $+\lambda_r \times \frac{1}{N}\sum_{i=1}^{N} ReLU(\epsilon_r - 0.385047574)$
PICNN5	$CCELoss(y_{true}, y_{pred})$ $+\lambda_t \times \frac{1}{N}\sum_{i=1}^{N} ReLU(\epsilon_t - 1.53658168)$ $+\lambda_r \times \frac{1}{N}\sum_{i=1}^{N} ReLU(\epsilon_r - 0.385047574)$

Key

- **R** = residual maximum melt pool temperature
- **l** = observed melt pool length
- **w** = observed melt pool width
- **N** = number of images
- ϵ_r = normalized percent error between empirical melt pool length:width ratio and simulated melt pool length:width ratio
- ϵ_t = normalized percent error between empirical maximum melt pool temperature and simulated maximum melt pool temperature
- λ_t = temperature-informed term scaling coefficient
- λ_r = length-to-width-ratio-informed term scaling coefficient

Performance Metrics

$$Accuracy = \frac{TP + TN}{TP + FP + TN + FN} \times 100 \quad (6)$$

$$Precision\ (weighted\ average) = (0.05 \times \frac{TP}{TP + FP} + 0.95 \times \frac{TN}{TN + FN}) \times 100 \quad (7)$$

$$Recall\ (weighted\ average) = (0.05 \times \frac{TP}{TP + FN} + 0.95 \times \frac{TN}{TN + FP}) \times 100 \quad (8)$$

- TP (true positive) = # of correctly identified “bad” images
- TN (true negative) = # of correctly identified “good” images
- FP (false positive) = # of “good” images incorrectly labeled “bad”
- FN (false negative) = # of “bad” images incorrectly labeled “good”

Baseline (Deep Learning-Only) Model Performance

- Training session parameters
  - Epochs = 100 (val. loss patience of 50)
  - Learning rate = 0.001
  - Stochastic gradient descent (SGD) optimizer
  - Categorical cross entropy loss function
- Best weights (based on lowest validation loss) from each training session were used to generate predictions
- Training set performance
  - 98.86% accuracy
  - 99% precision (weighted average)
  - 99% recall (weighted average)
- Test set performance
  - 93.87% accuracy
  - 91% precision (weighted average)
  - 94% recall (weighted average)

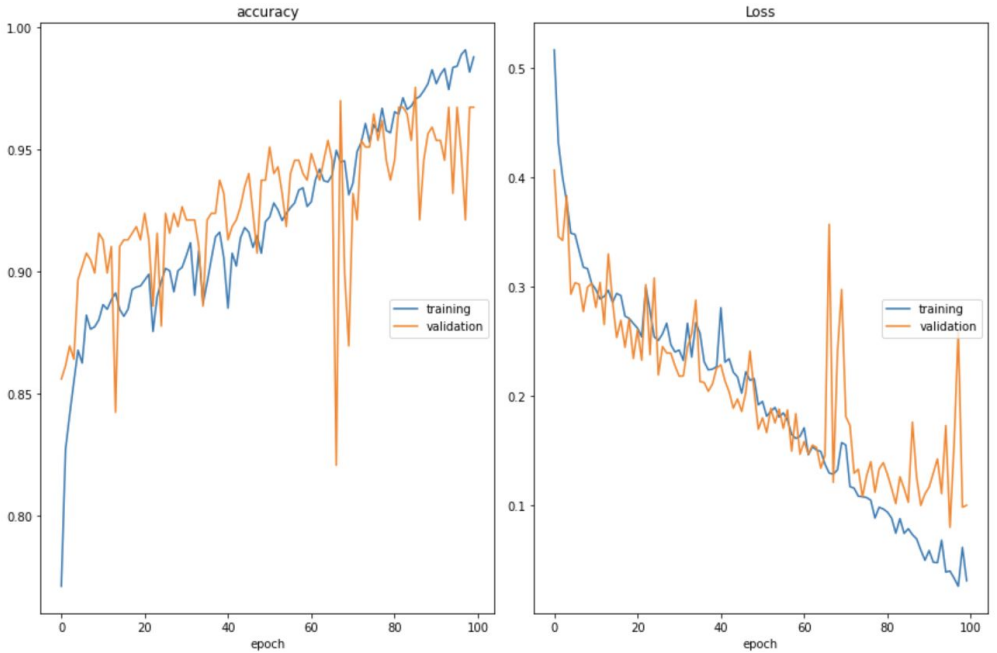

Fig. 6: Live accuracy (left) and loss (right) plots from the baseline model training session

Physics-Informed Models Performance

Model	λ_t	λ_r	Accuracy (%)	Precision (%) (Weighted Avg.)	Recall (%) (Weighted Avg.)
Deep Learning Only	-	-	93.87	91	94
PICNN1	-	-	88.89	91	89
PICNN2	-	-	88.51	91	89
PICNN3	1	-	87.36	91	87
	0.5	-	91.57	92	92
	0.05	-	89.27	91	89
PICNN4	-	1	86.97	91	87
	-	0.5	79.31	92	79
	-	0.05	72.80	92	73
PICNN5	0.5	1	91.57	91	92

Table 1: Performance metrics for the baseline deep learning-only model and each version of the physics-informed model when tested on the test dataset

Physics-Informed Models Performance (cont.)

Model	λ_t	λ_r	TP	TN	FP	FN
Deep Learning Only	-	-	0	245	4	12
PICNN1	-	-	1	231	18	11
PICNN2	-	-	1	230	19	11
PICNN3	1	-	1	227	22	11
	0.5	-	1	238	11	11
	0.05	-	1	232	17	11
PICNN4	-	1	1	226	23	11
	-	0.5	3	204	45	9
	-	0.05	4	186	63	8
PICNN5	0.5	1	0	239	10	12

Table 2: The number of true positive (TP), true negative (TN), false positive (FP), and false negative (FN) predictions for the baseline deep learning-only model and each version of the physics-informed model when tested on the test dataset

Conclusions

- Key findings:
  - While this physics-informed model was not able to improve the predictive capabilities of the deep learning model in every respect, some versions were able to improve upon the precision of the baseline model
  - This improvement in precision
    - Was due to an increase in the number of true positive predictions
    - Came at the expense of the overall accuracy of the model
- With these preliminary findings in mind, we will continue to explore and seek to maximize the effectiveness of incorporating both empirical and simulated melt pool data into a deep learning porosity prediction model

References

[1] M. Schmidt, M. Merklein, D. Bourell, D. Dimitrov, T. Hausotte, K. Wegener, L. Overmeyer, F. Vollertsen, G. N. Levy, Laser based additive manufacturing in industry and academia, CIRP Annals 66 (2) (2017) 561–583. doi:https://doi.org/10.1016/j.cirp.2017.05.011. URL https://www.sciencedirect.com/science/article/pii/S0007850617301506

[2] W. Guo, Q. Tian, S. Guo, Y. Guo, A physics-driven deep learning model for process-porosity causal relationship and porosity prediction with interpretability in laser metal deposition, CIRP Annals - Manufacturing Technology 69 (1) (2020) 205–208, publisher Copyright: © 2020 CIRP. doi:10.1016/j.cirp.2020.04.049.

[3] Q. Tian, S. Guo, E. Melder, L. Bian, W. Guo, Deep learning-based data fusion method for in situ porosity detection in laser-based additive manufacturing, Journal of Manufacturing Science and Engineering 143 (2021). doi:10.1115/1.4048957. URL https://doi.org/DOI: 10.1115/1.4048957

[4] B. Kapusuzoglu, S. Mahadevan, Physics-informed and hybrid machine learning in additive manufacturing: Application to fused filament fabrication, JOM 72 (2020). doi:10.1007/s11837-020-04438-4. URL https://doi.org/10.1007/s11837-020-04438-4

[5] A. Karpatne, W. Watkins, J. Read, V. Kumar, Physics-guided neural networks (pgnn): An application in lake temperature modeling (2018). arXiv:1710.11431.

[6] G. J. Marshall, S. M. Thompson, N. Shamsaei, Data indicating temperature response of ti–6al–4v thin-walled structure during its additive manufacture via laser engineered net shaping, Data in Brief 7 (2016) 697–703. doi:https://doi.org/10.1016/j.dib.2016.02.084. URL https://www.sciencedirect.com/science/article/pii/S2352340916301081

[7] M. Khanzadeh, S. Chowdhury, M. Marufuzzaman, M. A. Tschopp, L. Bian, Porosity prediction: Supervised-learning of thermal history for direct laser deposition, Journal of Manufacturing Systems 47 (2018) 69–82. doi:https://doi.org/10.1016/j.jmsy.2018.04.001. URL https://www.sciencedirect.com/science/article/pii/S0278612518300402

[8] V. Gawade, V. Singh, W. Guo, Leveraging simulated and empirical data-driven insight to supervised-learning for porosity prediction in laser metal deposition, Manuscript in Preparation (2021).

[9] G. Welsch, R. Boyer, E. Collings, Materials properties handbook: Titanium alloys (1993).

[10] K. Simonyan, A. Zisserman, Very deep convolutional networks for largescale image recognition (2015). arXiv:1409.1556.

Thank you to Dr. Guo, her graduate student Vidita Gawade, and the DIMACS REU Program for your support and guidance on this project.

Thank you as well to the National Science Foundation; this work is supported by NSF grant CCF-1852215.